

Nonvolatile resistive switching in metal/La-doped BiFeO₃/Pt sandwiches

Mi Li, Fei Zhuge, Xiaojian Zhu, Kuibo Yin, Jinzhi Wang, Yiwei Liu, Congli He, Bin Chen and Run-Wei Li¹

Ningbo Institute of Materials Technology and Engineering (NIMTE), Chinese Academy of Sciences (CAS), Ningbo 315201, People's Republic of China

E-mail: runweili@nimte.ac.cn

Received 13 May 2010, in final form 2 September 2010

Published 22 September 2010

Online at stacks.iop.org/Nano/21/425202

Abstract

The resistive switching (RS) characteristics of a Bi_{0.95}La_{0.05}FeO₃ (La-BFO) film sandwiched between a Pt bottom electrode and top electrodes (TEs) made of Al, Ag, Cu, and Au have been studied. Devices with TEs made of Ag and Cu showed stable bipolar RS behaviors, whereas those with TEs made of Al and Au exhibited unstable bipolar RS. The Ag/La-BFO/Pt structure showed an on/off ratio of 10², a retention time > 10⁵ s, and programming voltages < 1 V. The RS effect can be attributed to the formation/rupture of nanoscale metal filaments due to the diffusion of the TEs under a bias voltage. The maximum current before the reset process (on-to-off switching) was found to increase linearly with the current compliance applied during the set process (off-to-on switching).

(Some figures in this article are in colour only in the electronic version)

1. Introduction

As a candidate for nonvolatile memory devices, resistive random access memory (RRAM) based on the resistive switching (RS) effect has attracted great attention due to its superior characteristics, such as high operation speed, high storage density, and low power consumption [1]. A large variety of solid-state materials exhibit the RS effect, including organic materials [2, 3], binary oxides [4, 5], amorphous Si [6], carbon-based materials [7–9], and complex perovskite oxides such as Pr_{1-x}Ca_xMnO₃ [10], La_{1-x}Ca_xMnO₃ [11], and La₂CuO_{4+x} [12]. To elucidate the RS behaviors in complex perovskite oxides, various mechanisms have been proposed. Odagawa *et al* [13] suggested that the RS of Ag/Pr_{0.7}Ca_{0.3}MnO₃/Pt heterostructures induced by current-voltage (*I*-*V*) hysteresis should be attributed to the bulk limited conduction transition between the trap-filled space charge limited conduction (SCLC) and the trap-unfilled SCLC. Shang *et al* [14] found that the RS of Au/SrTiO₃:Nb Schottky junctions is closely related to electron tunneling. However, Hamaguchi *et al* [15] pointed out that the RS of perovskite oxides is not dominated by a detailed electronic structure of

each sample, but dominated by a more general origin, e.g., crystalline defect.

Recently, RS behaviors have been observed in Ca-doped BiFeO₃ films by conducting atomic force microscopy, which were suggested to result from the creation/erasure of a p-n junction due to nonhomogeneously distributed oxygen vacancies [16]. BiFeO₃ is one of the most important single-phase multiferroic materials with high ferroelectric and antiferromagnetic ordering temperatures [17, 18]. Doping at the Bi site could improve the crystallization and reduce the leakage of BiFeO₃ [19]. Sandwiching BiFeO₃ between two ferromagnetic metals may result in tunneling magnetoresistance and electroresistance which could be controlled both by electric and magnetic fields, giving rise to a four-state memory device [20–22]. Therefore, BiFeO₃ is a very important information storage material for fabricating future high-density magneto-electric random access memory. However, until now the RS effect of the metal/BiFeO₃/metal sandwiched structure has not been investigated, though the sandwiched structure is very important for real technical applications. In this paper, we have studied the RS characteristics in metal/Bi_{0.95}La_{0.05}FeO₃/Pt sandwiched structures, and observed bipolar RS behaviors which can be attributed to the formation/rupture of nanoscale metal filaments due to the diffusion of the top electrodes (TEs) under a bias

¹ Author to whom any correspondence should be addressed.

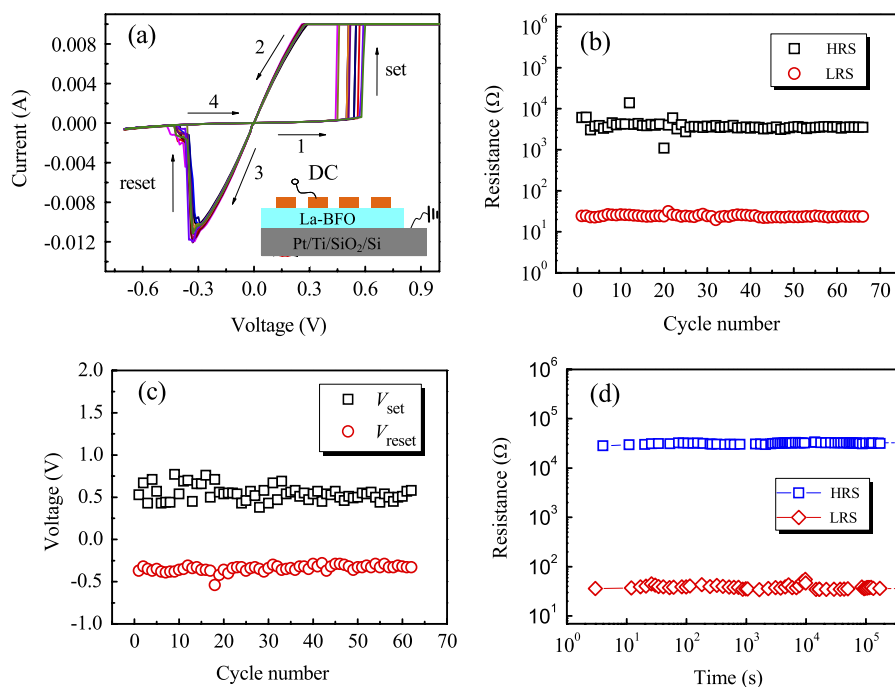


Figure 1. (a) Typical I - V characteristics of the Ag/La-BFO/Pt structure; the inset shows the schematic configuration of the device; (b) the endurance performance; (c) the distributions of the programming voltages (V_{set} and V_{reset}); and (d) retention for the LRS and HRS of the Ag/La-BFO/Pt device at RT.

voltage. The effects of the current compliance applied during the set process (off-to-on switching) and TE material on the switching properties were also investigated.

2. Experimental details

$\text{Bi}_{0.95}\text{La}_{0.05}\text{FeO}_3$ (La-BFO) films were prepared by the sol-gel method on commercial Pt/Ti/SiO₂/Si substrates. $\text{Bi}(\text{NO}_3)_3 \cdot 5\text{H}_2\text{O}$, $\text{La}(\text{NO}_3)_3 \cdot n\text{H}_2\text{O}$, and $\text{Fe}(\text{NO}_3)_3 \cdot 9\text{H}_2\text{O}$ were used as starting materials to prepare the precursor solution. Excess 2 mol% $\text{Bi}(\text{NO}_3)_3 \cdot 5\text{H}_2\text{O}$ was used to attempt to compensate for the expected loss of volatile Bi during the following heat treatment. The films were deposited by spin coating at 5000 rpm for 30 s and then preheated at 300 °C for 10 min to remove volatile materials. The above spin coating and preheating procedure was repeated until the desired film thickness was achieved. Finally, the films were annealed at 700 °C for 10 min at air ambient. The thickness of the films was about 300 nm. X-ray diffraction (XRD) patterns indicated that the as-grown films are of a perovskite structure. The cross-sectional transmission electron microscopy (TEM) observations showed that the films are polycrystalline. The atomic force microscopy (AFM) measurements showed that the average surface roughness of the films is about 7.8 nm. In order to measure the electrical properties, metal TEs with a thickness of 200 nm and diameter of 100 μm were deposited at room temperature (RT) by electron beam evaporation with an *in situ* metal shadow mask. The I - V characteristics of metal/La-BFO/Pt structures were measured at RT using a Keithley 4200 semiconductor characterization system with voltage sweeping mode. The sweeping step is 0.01 V, and the

sweeping speed is normal. During the measurement, a bias voltage was applied between the top and bottom (Pt) electrodes with the latter being grounded. The resistances in the on and off states of the metal/La-BFO/Pt structures were measured as a function of temperature by a physical property measurement system (PPMS, Quantum Design).

3. Results and discussion

Figure 1(a) shows the typical I - V characteristics of Ag/La-BFO/Pt structures. The schematic structure of the devices is depicted in the inset of figure 1(a). No forming process was necessary to initiate the switching property of the Ag/La-BFO/Pt devices. When the positive voltage is increased, the devices switch from the high resistance state (HRS or off state) to a low resistance state (LRS or on state) at about 0.5 V (set voltage). A current compliance (I_{comp} , 10 mA in this work) is usually needed during the set process to prevent the sample from a permanent breakdown. When the voltage sweeps to negative values, the devices switch back to the HRS at about -0.35 V (reset voltage). The I - V characteristics exhibit a typical nonvolatile switching behavior.

The resistance evolutions of the HRS and LRS of the Ag/La-BFO/Pt memory cells are shown in figure 1(b). The resistance ratio between HRS and LRS is more than two orders of magnitude. Although there is a slight fluctuation of resistances in the LRS and HRS (R_{LRS} and R_{HRS}), a stable switching property is observed. Figure 1(c) shows the evolutions of the programming voltages (V_{set} and V_{reset}). V_{set} and V_{reset} distribute in a range of 0.4 to 0.8 V and -0.3 to -0.5 V, respectively. The switching threshold voltages of the

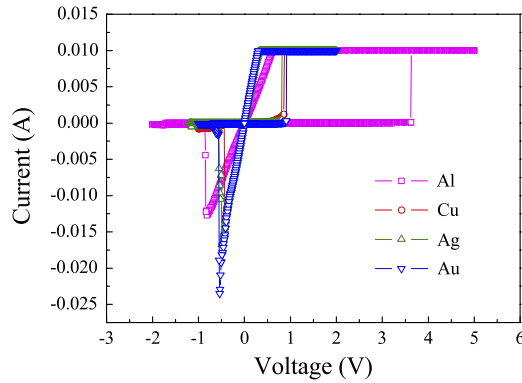


Figure 2. I - V characteristics for Al/La-BFO/Pt, Ag/La-BFO/Pt, Cu/La-BFO/Pt, and Au/La-BFO/Pt.

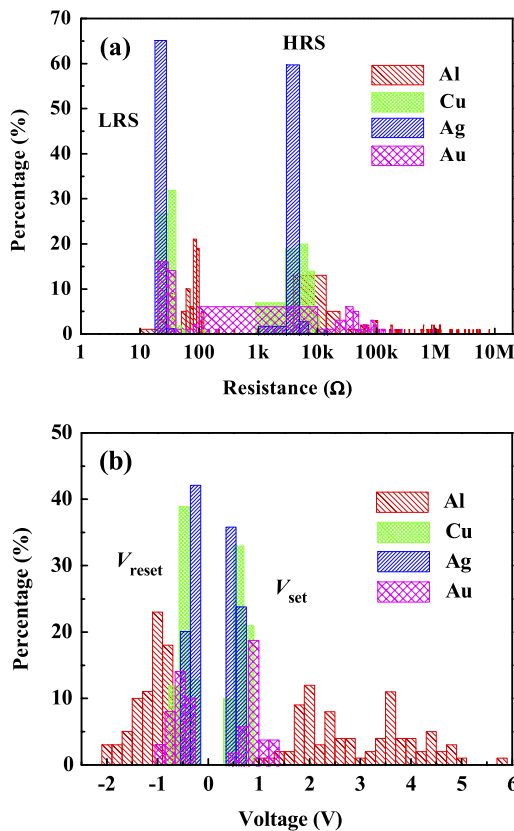


Figure 3. Statistical distributions of (a) the resistances in HRS and LRS, and (b) programming voltages (V_{set} and V_{reset}) of the metal/La-BFO/Pt devices with different top electrodes (Al, Cu, Ag, and Au).

Ag/La-BFO/Pt devices are lower than those of most reported RRAM devices [4–6, 10–12]. The retention characteristic of the devices is shown in figure 1(d). The device was switched on or off by dc voltage sweeping. Then R_{LRS} or R_{HRS} was read out at a reading voltage of 0.1 V. No significant changes in the resistances for 2×10^5 s can be observed at RT, indicating that the device is nonvolatile and stable at RT. The results indicate that the Ag/La-BFO/Pt device is a promising candidate for memristor applications.

To investigate the switching mechanism of the metal/La-BFO/Pt memory cells, different metals (Al, Ag, Cu, and Au)

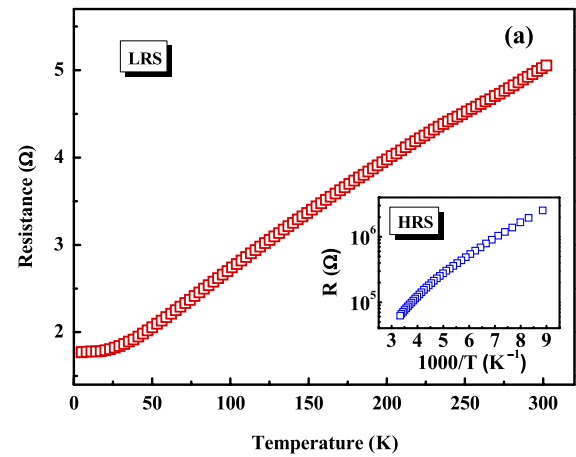


Figure 4. (a) Temperature dependence of the resistance in the LRS of the Ag/La-BFO/Pt device; the inset shows the temperature dependence of the resistance in the HRS; (b) device-area dependence of the resistances of LRS and HRS for the Ag/La-BFO/Pt device.

were used as TEs. All the memory cells with different TEs were found to show bipolar RS phenomena, as shown in figure 2. Tokunaga *et al* [23] investigated the RS effect at the interface between metal electrodes (Pt, Au, Ag, Al, Ti, and Mg) and atomically flat cleaved (001) surfaces of $\text{La}_{1-x}\text{Sr}_{1+x}\text{MnO}_4$ ($x = 0-1.0$) single crystals. Hysteretic I - V characteristics were observed in the junctions for Mg, Al, and Ti, which have relatively shallow work functions (Φ). In our case, compared to La-BFO ($\Phi = 4.7$ eV), Al, Cu, and Ag have a lower Φ of 4.28 eV, 4.35 eV, and 4.26 eV, respectively, whereas Au has a higher one of 5.1 eV. It indicates that the occurrence of the RS in metal/La-BFO/Pt structures is irrelevant to Φ of the TEs. Liao and co-workers [24] studied the RS characteristics of metal/ $\text{Pr}_{0.7}\text{Ca}_{0.3}\text{MnO}_3$ (PCMO)/Pt devices and found that devices with TEs made of Al, Ti, and Ta exhibit a bipolar RS, but those with TEs made of Pt, Ag, Au, and Cu do not. The RS was attributed to a thin metal-oxide layer formed at the interface between the former group of TEs and PCMO. In our work, the TE material includes both reactive metals such as Al and inert metals such as Au. Therefore, the observed RS is not due to the formation of a metal-oxide layer at the interface between the TE and La-BFO. Figures 3(a) and (b) show the

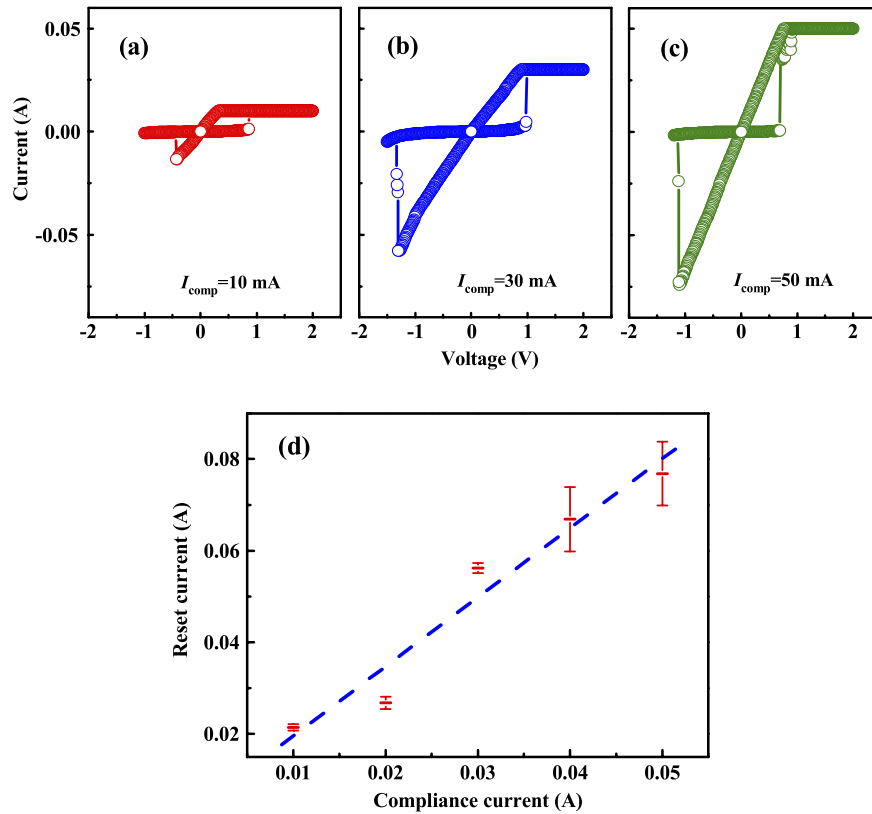


Figure 5. (a)–(c) Typical I – V characteristics of the Ag/La-BFO/Pt device with different current compliances ($I_{\text{comp}} = 10, 30,$ and 50 mA), and (d) current compliance dependence of the reset current. The sweeping step is 0.01 V, and the sweeping speed is normal.

statistical distributions of the resistances in HRS and LRS, and programming voltages of memory cells with different TEs, respectively. From figure 3, we see that compared to the devices with Al and Au as TEs, the devices with Ag and Cu TEs exhibit much more stable RS behaviors and much lower programming voltages. The strong TE material dependence of the switching characteristics suggests that the RS effect may be attributed to the formation/rupture of metal filaments due to the diffusion of the TEs under a bias voltage. Briefly, a positive voltage ($>V_{\text{set}}$) on the TEs generates a high electric field that drives metal (e.g., Ag) ions into the La-BFO matrix and forms conducting filaments inside the La-BFO layer, and the device reaches the on state. After the set process, the device retains the on state unless a sufficient voltage of opposite polarity ($<V_{\text{reset}}$) is applied and the electrochemical dissolution of the metal filaments resets the device, and the off state is finally reached again [8]. The unstable RS observed in Al/La-BFO/Pt devices is likely due to the formation of a thin AlO_x layer at the interface between the TE and La-BFO which is detrimental to the Al ion diffusion, whereas in the case of using Au as the TE, the unstable RS may be due to a large ionic radius of Au which makes the Au ion diffusion difficult in the La-BFO matrix.

To verify the physical nature of the RS effect of the metal/La-BFO/Pt structures, R_{LRS} and R_{HRS} of the Ag/La-BFO/Pt device were measured as a function of temperature. Figure 4(a) shows the typical metallic behavior of R_{LRS} . In contrast, R_{HRS} shows a semiconducting behavior as displayed in the inset of figure 4(a). The metallic conducting behavior

in the LRS indicates the formation of conducting filaments in the La-BFO films. Furthermore, R_{HRS} clearly increases with a decrease of the device area; however, R_{LRS} shows weak dependence on the device area, as shown in figure 4(b). The area-insensitive property of R_{LRS} further confirms that the RS of the Ag/La-BFO/Pt device is dominated by the conducting-filament mechanism [25]. The temperature dependence of metallic resistance can be written as $R(T) = R_0[1 + \alpha(T - T_0)]$, where R_0 is the resistance at temperature T_0 , and α is the temperature coefficient of resistance. By choosing T_0 as 300 K, the α of the filaments is calculated to be $2.4 \times 10^{-3} \text{ K}^{-1}$, which matches excellently with the value $2.5 \times 10^{-3} \text{ K}^{-1}$ for Ag nanowires of diameter ≥ 15 nm [26]. Considering the fact that the temperature coefficients of all other involved elements and compounds are distinctly different from the measured value, we conclude that the metallic behavior of the LRS originates from the conducting Ag filaments with a size of about tens of nanometers due to the diffusion of the TEs under a bias voltage.

Figures 5(a)–(c) show the I – V characteristics of the Ag/La-BFO/Pt memory cells with different I_{comp} of 10, 30, and 50 mA. The reset current (maximum current level before the reset process) is found to increase obviously with increasing I_{comp} . It was considered that stronger filaments with a higher density are formed at a larger I_{comp} [27]. The reset process was also considered to be due to the rupture of the filaments due to the heat generated by the large current flow [27]. Thus, it can be imagined that a larger reset current is necessary for the reset process at the larger I_{comp} . The reset current has

an approximately linear relationship to the I_{comp} , as shown in figure 5(d). Therefore, the power needed for the WRITE and ERASE operations in RRAM can be modulated by controlling the current compliance.

4. Summary

In summary, reliable and reproducible resistance switching behaviors were observed in metal/La-BFO/Pt sandwiched devices. The resistance ratio between the HRS and LRS of the Ag/La-BFO/Pt device was about 100. The device exhibited good retention characteristics and low switching voltages. The reset current was found to show a linear dependence on the current compliance. Thus, the switching power in RRAM can be modulated by controlling the current compliance. The observed switching effect could be attributed to the formation/rupture of nanoscale metal filaments due to the diffusion of the TEs.

Acknowledgments

The authors acknowledge the financial support from Chinese Academy of Sciences (CAS), State Key Project of Fundamental Research of China (973 Program), National Natural Science Foundation of China, Zhejiang Qianjiang Talent Project, Zhejiang and Ningbo Natural Science Foundations.

References

- [1] Meijer G I 2008 *Science* **319** 1625
- [2] Stewart D R, Chen Y, Williamms R S, Jeppesen J O, Nielsen K A and Stoddart F 2004 *Nano Lett.* **4** 133
- [3] Ma L P, Pyo S, Ouyang J, Xu Q and Yang Y 2003 *Appl. Phys. Lett.* **82** 1419
- [4] Liu M, Abid Z, Wang W, He X L, Liu Q and Guan W H 2009 *Appl. Phys. Lett.* **94** 233106
- [5] Schindler C, Staikov G and Waser R 2009 *Appl. Phys. Lett.* **94** 072109
- [6] Jo S H, Kim K H and Lu W 2009 *Nano Lett.* **9** 870
- [7] Li Y B, Sinitskii A and Tour J M 2008 *Nat. Mater.* **7** 966
- [8] Zhuge F, Dai W, He C L, Wang A Y, Liu Y W, Li M, Wu Y H, Cui P and Li R W 2010 *Appl. Phys. Lett.* **96** 163505
- [9] He C L et al 2009 *Appl. Phys. Lett.* **95** 232101
- [10] Liu S Q, Wu N J and Ignatiev A 2000 *Appl. Phys. Lett.* **76** 2749
- [11] Hasan M, Dong R, Choi H J, Lee D S, Seong D J, Pyun M B and Hwang H 2008 *Appl. Phys. Lett.* **92** 202102
- [12] Hamaguchi M, Aoyama K, Asanuma S, Uesu Y and Katsufuji T 2006 *Appl. Phys. Lett.* **88** 142508
- [13] Odagawa A, Sato H, Inoue I H, Akoh H, Kawasaki M, Tokula Y, Kanno T and Adachi H 2004 *Phys. Rev. B* **70** 224403
- [14] Shang D S, Sun J R, Shi L, Wang J, Wang Z H and Shen B G 2009 *Appl. Phys. Lett.* **94** 052105
- [15] Hamaguchi M, Aoyama K, Asanuma S, Uesu Y and Katsufuji T 2006 *Appl. Phys. Lett.* **88** 142508
- [16] Yang C H et al 2009 *Nat. Mater.* **8** 485
- [17] Ramesh R and Spaldin N A 2007 *Nat. Mater.* **6** 21
- [18] Cheong S W and Mostovoy M 2007 *Nat. Mater.* **6** 13
- [19] Singh S K, Maruyama K and Ishiwara H 2007 *J. Phys. D: Appl. Phys.* **40** 2705
- [20] Bea H, Gajek M, Bibes M and Barthelemy A 2008 *J. Phys.: Condens. Matter* **20** 434221
- [21] Bea H et al 2006 *Appl. Phys. Lett.* **89** 242114
- [22] Catalan G and Scott J F 2009 *Adv. Mater.* **21** 2463
- [23] Tokunaga Y, Kaneko Y, He J P, Arima T, Sawa A, Fuji T, Kawasaki M and Tokura Y 2006 *Appl. Phys. Lett.* **88** 223507
- [24] Liao Z L, Wang Z Z, Meng Y, Liu Z Y, Gao P, Gang J L, Zhao H W, Liang X J, Bai X D and Chen D M 2009 *Appl. Phys. Lett.* **94** 253503
- [25] Liu Q, Long S B, Wang W, Zuo Q Y, Zhang S, Chen J N and Liu M 2009 *IEEE Electron Device Lett.* **30** 1335
- [26] Bid A, Bora A and Raychaudhuri A K 2006 *Phys. Rev. B* **74** 035426
- [27] Rohde C, Choi B J, Jeong D S, Choi S, Zhao J S and Hwang C S 2005 *Appl. Phys. Lett.* **86** 262907